KSME International Journal, Vol. 16 No. 3, pp. 283~291, 2002

An Application of Sliding Horizon Control to an Electro-Hydraulic Automotive Seat Simulator

Changki Mo*
School of Mechanical Engineering, SangJu National University, Kyungbuk 742-711, Korea
Myoungho Sunwoo
Department of Automotive Engineering, Hanyang University, Seoul 133-791, Korea
Wenzhen Yan
Former Graduate Student in Controls Lab., University of Oklahoma, OK 73019, U.S.A.

The paper demonstrates the tracking performance of a sliding horizon feedback/feedforward preview optimal control when applied to a hydraulic motion simulator which has been built to provide a means of replicating the actual ride dynamics of an automobile seat/human system. The design was developed by solving an ordinary differential equation problem instead of a Ricatti equation. Simulation results indicate that the proposed technique has good performance improvement in phase tracking when compared to the classical design methods. It is also found that the controller can be adjusted more easily for robustness due to more tuning parameters.

Key Words: Sliding Horizon Control, Feedforward, Seat Motion Simulator, Robustness, Tracking Performance

1. Introduction

Automotive motion simulators require to reproduce the dominant vibration modes of motion experienced by a rider in the vehicle. Traditional control designs for simulators are not able in general to meet the strict requirements for flat magnitude and phase response over the specified bandwidth of the simulator. A control technique described here produces a feedback/feedforward controller for a simulator that makes it possible to track a command with fidelity.

The application of the sliding horizon control approach, which belongs to a class of model based predictive control techniques, is described in the paper. The various model based predictive control algorithms in general differ in the models used to represent a process, and the cost functions to be minimized. Sliding horizon control is based on a state space representation of the model. It allows straightforward generalization to multivariable systems which are of interest in industrial applications.

In most tracking control problems, the path to be followed over a finite future length of time (the horizon length) is available. A control using prior knowledge of the path, or command input is often called preview control (Cho, 1999). Recent research has been aimed at developing methods that provide tracking when the desired trajectory is known only over a finite future interval of time. Tomizuka and Rosenthal (1979) have demonstrated that the application of the quadratic regulator to a system with anticipative inputs can provide improved performance. Lee, Bien, and Park (1990) describe the use of an instantaneous optimal controller that results in one step ahead tracking design for an aircraft. Kwon, Byun, and Noh (1989; 1992) have examined the use of an optimal receding horizon control design for tracking and disturbance rejection. However,

* Corresponding Author,
E-mail : ckmo@sangju.ac.kr
TEL : +82-54-530-5405; **FAX** : +82-54-530-5407
School of Mechanical Engineering, SangJu National University, 386, Gajang-dong, Sangju, Kyungbuk 742-711, Korea. (Manuscript **Received** July 29, 2000; **Revised** November 30, 2001)

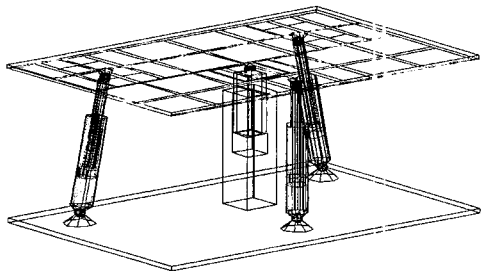

Fig. 1 Kinematic representation of the seat simulator assembly

their design requires the real-time solution of a Ricatti type equation. The development of a sliding horizon controller with fixed gains based on the approximation of the finite time LQR is first discussed in Patten (Patten et al., 1993; 1994).

The proposed design is developed by solving a linear ordinary differential equation problem instead of solving a Ricatti equation. Simulation results indicate the fact that while conventional designs do provide good tracking of the magnitude of the command reference, they provide very poor tracking of the phase characteristics of the command. The severe phase delay made it impossible to accurately produce a real road profile using the simulator.

2. Model Description

One type of seat simulator that can replicate three degree of ride motion has been examined (Kuo et al., 1993; Kuehn et al., 1993; Shen et al., 1996). The simulator is an parallel kinematic mechanism restrained by a center post and powered by three hydraulic actuators which combine to provide pitch, roll and heave motion enabling it to reproduce most of the predominant movements experienced in an automobile. The simulator system is expected to be able to track virtually any reference seat track trajectory using only partial state feedback. The kinematic representation of the platform, actuators and restraining center post is depicted in Fig. 1.

An analytic model of the platform dynamics has been developed by Kuo (Kuo et al., 1993). A

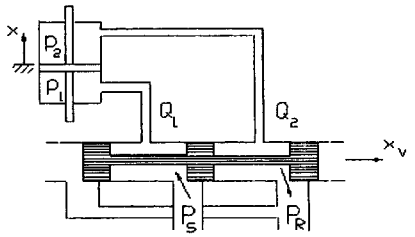

Fig. 2 Scheme of a servo-actuating system

control design based on a full nonlinear model of the system is possible but impractical. A practical controller design for the simulator is possible if the actuators are treated as independent joint controllers. If the operation of the simulator is restricted to the vertical motion, the system can be treated as three independent actuator systems.

Referring to the scheme of a servo-actuating system (Fig. 2), the flow equation across the valve is

$$Q_L = C_d W X_v \sqrt{\frac{1}{\rho}(P_s - \Delta P)} \tag{1}$$

where, C_d is discharge coefficient, WX_v is the open area of the valve orifice, P_s is supply pressure, ρ is fluid density, and $\Delta P (= P_1 - P_2)$ is differential pressure.

The flow equation can be linearized by considering a small perturbation about a working position as follows.

$$Q_L = k_q X_v - k_c \Delta P \tag{2}$$

Where, k_q is the flow gain and k_c is the flow-pressure coefficient. Considering the fluid compressibility and leakage, the flow equation becomes

$$Q_L = C_t \Delta P + A_p \dot{x} + \frac{V_t}{4\beta} \Delta \dot{P} \tag{3}$$

where C_t is the total leakage coefficient, A_p is the effective area of the cylinder, V_t is the total volume of the cylinder, and β is bulk modulus.

Eqs. (2) and (3) can be rewritten as

$$\Delta \dot{P} = \frac{4\beta}{V_t}[-(C_t + k_c)\Delta P - A_p \dot{x} + k_q X_v] \tag{4}$$

Neglecting the valve delay, then

$$X_v = K_i K_u u \tag{5}$$

where K_i is the gain of the stroke of the valve

spool X_v over the input current i, and K_u is the gain of the input current i over the input voltage u.

Substituting Eq. (5) into (4)

$$\dot{\Delta P}=\frac{4\beta}{V_t}[-(C_t+k_c)\Delta P-A_p\dot{x}+k_qK_iK_uu] \quad (6)$$

By the Newton's second law, the resulting force equation is

$$A_p\Delta P=m_e\ddot{x}+c_e\dot{x}+k_ex \quad (7)$$

where, m_e is mass, c_e and k_e are equivalent damping ratio and stiffness of the actuator system.

If the states are defined as $X_1=x$, $X_2=\dot{x}$, and $X_3=\Delta P$, then the state space representation of the model becomes:

$$\dot{X}=A_aX+B_au,\ y=C_aX \quad (8)$$

where,

$$A_a=\begin{Bmatrix} 0 & 1 & 0 \\ -\frac{k_e}{m_e} & -\frac{c_e}{m_e} & -\frac{A_p}{m_e} \\ 0 & -\frac{4\beta}{V_t} & -\frac{4\beta}{V_t}(C_t+k_c) \end{Bmatrix},$$

$$B_a=\begin{Bmatrix} 0 \\ 0 \\ \frac{4\beta}{V_t}k_qK_tK_u \end{Bmatrix}, \text{ and } C_a=\begin{Bmatrix} 1 \\ 0 \\ 0 \end{Bmatrix}^T$$

Defining the states as $X_1=x$, $X_2=\dot{x}$, and $X_3=\ddot{x}$, then the state space representation of the model which utilized in this work becomes

$$\dot{X}=AX+Bu, \text{ and } y=CX \quad (9)$$

where

$$A=\begin{Bmatrix} 0 & 1 & 0 \\ 0 & 0 & 1 \\ -\frac{4\beta}{m_eV_t}(C_t+k_c)k_e & -\frac{4\beta}{m_eV_t}\left\{c_e(C_t+k_c)+\frac{V_tk_e}{4\beta}+A_p^2\right\} & -\frac{4\beta}{m_eV_t}\left\{m_e(C_t+k_c)+c_e\frac{V_t}{4\beta}\right\} \end{Bmatrix}$$

$$B=\begin{Bmatrix} 0 \\ 0 \\ \frac{4\beta}{m_eV_t}A_pk_qK_iK_u \end{Bmatrix}, \text{ and } C=(1\ 0\ 0)$$

Most parameters, such as V_t, A_p, K_i, and K_u can be physically measured. However, some parameters, such as β, C_t, and ρ may vary in the different working environments. Those parameters were estimated through experiment (Yan, 1994).

3. Controller Design

The goal is to construct a stable suboptimal feedback/feedforward control by means of the closed-form solution of a sliding horizon optimal controller. A sliding horizon feedback/feedforward controller was proposed to be a reliable controller for the hydraulic actuators of the seat simulator. A quadratic performance measure is adopted with a finite horizon. Instead of solving differential Riccati equation, the optimal u is obtained by the closed-form solution (Yan, 1994).

Referring to Eq. (9), the control criterion considered here is:

$$\text{Minimize } J=\frac{1}{2}\int_0^{T_f}(e^TQe+u^TRu)\,dt$$

$$\text{subject to } \dot{X}=AX+Bu \text{ and } X(0)=X_0.$$

where, $e=X-r$ is the difference between states X and the desired command r, $X\in R^n$, $u\in R^m$, $A\in R^{n\times n}$, and $B\in R^{n\times m}$.

The preview length T_f is finite and specified in the above problem. The penalty matrix Q is assumed to be positive semi-definite and R be positive definite. This guarantees the convexity of the quadratic functional and the existence of its lower bound on the interval $t\in[0,\ T_f]$, for sufficiently large T_f. The straightforward minimization of the quadratic functional produces a set of first order necessary conditions and transversality conditions (Kirk, 1970). The first order necessary conditions are;

the state equations,

$$-\dot{X}+AX+Bu=0 \quad (10)$$

the co-state equations,

$$\dot{P}+QX+A^TP-Qr=0 \quad (11)$$

where $P\in R^n$ is the co-state variable vector and the associated control equations,

$$R^Tu+B^TP=0 \quad (12)$$

The transversality conditions are

$$X(0)=X_0,\ P(T_f)=0 \tag{13}$$

where $0\in R^n$. Introducing $W=[X\ P]^T$, then the necessary conditions take the form

$$\dot{W}=MW+N \tag{14}$$

where $W\in R^{2n}$, $M\in R^{2n\times 2n}$, and $N\in R^{2n}$

$$M\triangleq\begin{bmatrix} A & -BR^{-1}B^T \\ -Q & -A^T \end{bmatrix},\ N\triangleq[0\ \ Qr]^T$$

The solution method to the two point boundary value problem is described next.

3.1 A closed-form solution

Assuming that the eigenvalues of matrix M are all distinct, the following transformation can be adopted

$$W=VZ \tag{15}$$

where $V\in R^{2n\times 2n}$ is an invertible modal matrix of M and $Z\in R^{2n}$ is the transformation variable. Substituting Eq. (15) into Eq. (14) yields

$$\dot{Z}=\Lambda Z+V^{-1}N \tag{16}$$

where $\Lambda=V^{-1}MV$ is a diagonal matrix where the diagonal elements $\lambda_i (i=1, 2, 3, \cdots, 2n)$ are the unique eigenvalues of the matrix M. Employing the basic theory of ordinary differential equations, the general solution of the decoupled differential system Eq. (16) can be obtained as

$$Z(t)=S(t)\,(c+\int_0^t [VS(\tau)]^{-1}N(\tau)\,d\tau) \tag{17}$$

where $c\in R^{2n}$ is the integral constant vector, and $S(t)\in R^{2n\times 2n}$(the state transition operator) (Brogan, 1985) is a diagonal and invertible matrix whose entries are defined as

$$S_{ii}(t)=\exp(\lambda_i t) \text{ where i=1, 2, ..., 2n.}$$

The general solution of Eq. (16) is then

$$W(t)=VS(t)\,(c+\int_0^t [VS(\tau)]^{-1}N(\tau)\,d\tau) \tag{18}$$

The constant vector c can be determined using the boundary conditions (Eq. (13)). Substituting Eq. (13) into Eq. (18) yields

$$\begin{pmatrix} X_0 \\ \bar{0} \end{pmatrix}=\begin{pmatrix} V_{upper} \\ V_{lower}S(T_f) \end{pmatrix}c + \begin{pmatrix} 0 \\ V_{lower}S(T_f)\int_0^{T_f}[VS(\tau)]^{-1}N(\tau)\,d\tau \end{pmatrix} \tag{19}$$

where $V_{upper}\in R^{n\times 2n}$ and $V_{lower}\in R^{n\times 2n}$ represent the upper-half and lower-half substructures of the matrix V respectively. The following transformation is then possible.

$$H_C=L \tag{20}$$

where $H\in R^{2n\times 2n}$ and $L\in R^{2n}$ are defined as;

$$H\triangleq\begin{bmatrix} V_{upper} \\ V_{lower}S(T_f) \end{bmatrix},$$

$$L\triangleq\begin{bmatrix} X_0 \\ -V_{lower}S(T_f)\int_0^{T_f}[VS(\tau)]^{-1}N(\tau)\,d\tau \end{bmatrix}$$

Noting that matrix V is full rank and orthogonal, and $S(T_f)$ is positive definite. The matrix H is nonsingular and the constant vector c can be solved uniquely as

$$c=H^{-1}L \tag{21}$$

The closed form solution for Eq. (18) is then

$$W(t)=VS(t)\,(H^{-1}L + \int_0^t [VS(\tau)]^{-1}N(\tau)\,d\tau),\ t\in[0,\ T_f] \tag{22}$$

and the combination of Eq. (22) and Eq. (9) yields the open-loop optimal control as

$$u(t)=-R^{-1}B^T V_{lower}S(t)\,(H^{-1}L + \int_0^t [VS(\tau)]^{-1}N(\tau)\,d\tau) \tag{23}$$

In the receding horizon optimal preview control, the control law (Eq. (23)) is used for a short duration h. After the interval h, the initial condition X_0 and the previewable trajectory are updated and a new optimal control u(0) is computed over an interval of the same length but shifted by the interval h.

The instantaneous control can then be rewritten as the form with gain on the current state and the anticipated command as:

$$u(0)=K_xX_0+K_f\int_0^{T_f}[VS(\tau)]^{-1}N(\tau)\,d\tau \tag{24}$$

where the gains $K_x\in R^{m\times n}$ and $K_f\in R^{m\times n}$ are respectively defined as

$$K_x\triangleq -R^{-1}B^T V_{lower}(H^{-1})_{left} \tag{25}$$

$$K_f\triangleq R^{-1}B^T V_{lower}(H^{-1})_{right}V_{lower}S(T_f) \tag{26}$$

where the subscripts left and right attached to H^{-1} represent the left-half and right-half substructure

of matrix H^{-1} respectively.

When simulating the performance of the control, the updated value of the state is obtained using

$$X(h)=V_{upper}S(h)\,(H^{-1}L+\int_0^h[\,VS(\tau)\,]^{-1}N(\tau)\,d\tau \quad (27)$$

Recalling the definition of L, Eq. (27) can be rearranged as

$$X(h)=V_{upper}S(h)\,(H^{-1})_{left}X_0-V_{upper}S(h)\cdot(H^{-1})_{right}V_{lower}S(T_f)\int_0^{T_f}[\,VS(\tau)\,]^{-1}N(\tau)\,d\tau+V_{upper}S(h)\int_0^h[\,VS(\tau)\,]^{-1}N(\tau)\,d\tau \quad (28)$$

Observing that the desired trajectory is usually a set of discrete signals for real control systems, N can be treated as a series of step functions with constant value in each sampling interval. The integral terms in Eq. (28) can then be calculated as

$$\begin{aligned}&\int_{(i-1)h}^{ih}[\,VS(\tau)\,]^{-1}N(\tau)\,d\tau\\&=\int_{(i-1)h}^{ih}[\,VS(\tau)\,]^{-1}d\tau N(ih-h)\\&=S_iN(ih-h)\end{aligned} \quad (29)$$

where, i=1, 2, ···, n_t-1, and n_t is the total number of sampling points in $t\in[0,\ T_f]$ with uniform sampling interval h.

Defining $S_i\in R^{2n\times 2n}$ as the integral in the i^{th} interval and noting that $S(t)\equiv e^{At}$, it takes the following form:

$$\begin{aligned}S_i&\triangleq\int_{(i-1)h}^{ih}[\,VS(\tau)\,]^{-1}d\tau\\&=-A^{-1}[I-e^{Ah}]S(-ih)\,V^{-1}\end{aligned} \quad (30)$$

The integral term can then be rewritten as

$$\begin{aligned}\int_0^{T_f}[\,VS(\tau)\,]^{-1}N(\tau)\,d\tau&=\sum_{i=1}^{n_t-1}S_i\begin{bmatrix}0\\Qr(ih-h)\end{bmatrix}\\&=\sum_{i=1}^{n_t-1}(S_i)_{right}Qr(ih-h)\end{aligned} \quad (31)$$

where $(S_i)_{right}$ is the right-half substructure of the matrix Si.

Assuming that the sliding step for each horizon is the same as the sampling interval h, the closed-loop instantaneous control (Eq. (24)) can be rewritten as:

$$u_k=K_xX_k+\sum_{i=1}^{n_t-1}(K_f)_ir_{k+i-1} \quad (32)$$

where the subscript k indicates the time point corresponding to t=kh and $(K_f)_i\in R^{n\times n}$ is defined as:

$$(K_f)_i\triangleq K_f(S_i)_{right}Q \quad (33)$$

Similarly, Eq. (27) can be rewritten as the recursive form as:

$$X_{k+1}=A_kX_k+\sum_{i=1}^{n_t-1}C_ir_{k+i-1} \quad (34)$$

where $A_k\in R^{n\times n}$, $C_i\in R^{n\times m}$ are defined as:

$$A_k\triangleq V_{upper}S(h)\,(H^{-1})_{left} \quad (35)$$

$$C_i\triangleq V_{upper}S(h)\,[\delta_{1i}I-(H^{-1})_{right}V_{lower}S(T_f)\,](S_i)_{right}Q \quad (36)$$

where δ is a Delta function, and I is a unit matrix.

3.2 Tracking performance analysis

For the seat motion simulator, the most important feature is its ability to track a prescribed motion trajectory over specific bandwidth (30Hz) of operation. Thus, the frequency domain measure is especially important. Since the trajectories used for testing are usually random signals, a flat magnitude response of the closed-loop system is not enough to insure tracking fidelity. The controller must also provide essentially a flat phase response over the domain of desired operation. The closed-loop transfer function is derived for the purpose of the analysis of tracking performance. Taking the z transformation of Eq. (34), it follows that

$$X(z)=T_{X/r}r(z) \quad (37)$$

where the closed-loop transfer function $T_{X/r}$ is defined as

$$T_{X/r}\triangleq(zI-A_k)^{-1}\sum_{i=1}^{n_t-1}C_iz^{i-1} \quad (38)$$

where n_t is the total number of sampling points in $t\in[0,\ T_f]$.

Applying the design derived her to the motion simulator, the tracking performance is shown with the design parameters. The simulations tested the sensitivity of the design to changes in preview length T_f are depicted in Fig. 3 and Fig. 4. The results indicate that an increase in the

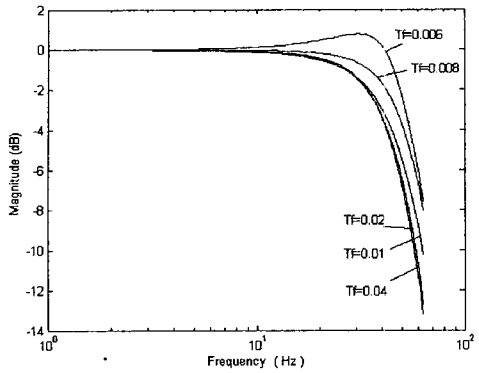

Fig. 3 Bode plot (magnitude) with different preview lengths

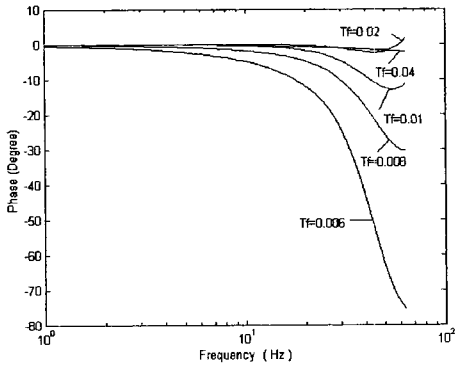

Fig. 4 Bode plot(phase) with different preview lengths

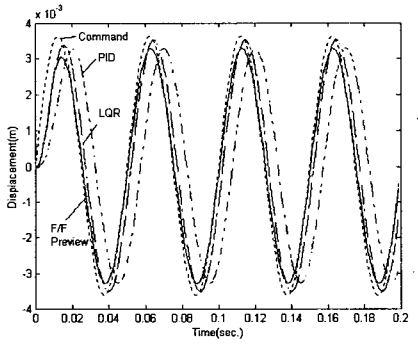

Fig. 5 Comparison of the simulated time responses to a sinusoidal command

preview length produces no obvious improvement for the magnitude tracking. However, an increase in T_f results in a decrease in phase lag. A comparison of the closed-loop time response to 20 Hz sinusoidal command is shown in Fig. 5. Figures 6

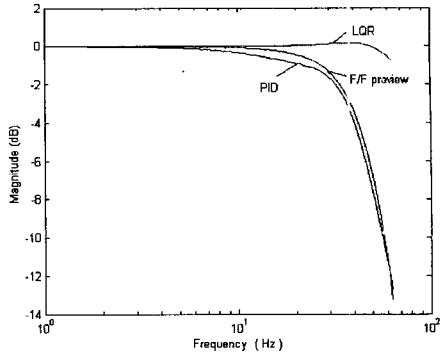

Fig. 6 Closed loop bode plot (magnitude)

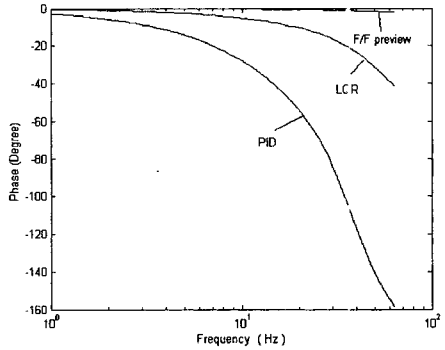

Fig. 7 Closed loop bode plot(phase)

and 7 depict simulation comparisons of the closed-loop Bode plot for the different control strategies. The results indicate that the sliding horizon feedback/feedforward preview optimal control design has good performance improvement in phase tracking comparing with PID and LQR, but the performance of the magnitude tracking is a little lower than LQR at higher frequencies.

3.3 Robustness analysis

An unavoidable fact in the design is that the nominal model being considered for control will differ in behavior from the actual system. It is because modeling of physical systems for control design invariably involves a trade-off between simplicity of the model and its accuracy in matching the behavior of the actual system.

3.3.1 Robust performance

Performance robustness ensures that the performance of the closed-loop system remains

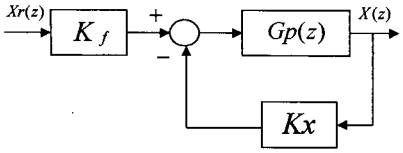

Fig. 8 A simplified block diagram of the closed-loop system

within specified bounds if the true process is different from the model. For robustness analysis a simplified block diagram for the proposed design is assumed as shown in Fig. 8.

Assumig $G_p(z)$ is transfer functions of the true plant, that is $G_P(z)=(zI-A)^{-1}B$, and $\hat{G}_P(z)$ is transfer functions of the nominal plant. The relative change of $\Delta_c(z)$ of the closed-loop transfer function describing the tracking behavior with respect to process changes is defined by

$$\Delta_c(z)=\frac{\dfrac{G_P(z)K_f}{1+G_P(z)K_x}-\dfrac{\hat{G}_P(z)K_f}{1+\hat{G}_P(z)K_x}}{\dfrac{G_P(z)K_f}{1+G_P(z)K_x}}$$
$$=\frac{G_P(z)-\hat{G}_P(z)}{G_P(z)}\cdot\frac{1}{1+\hat{G}_P(z)K_x}$$
$$=\Delta_o(z)\frac{1}{1+\hat{H}_L(z)} \tag{39}$$

where $\Delta_o(z)=\dfrac{G_P(z)-\hat{G}_P}{G_P(z)}$, and $\hat{H}_L=\hat{G}_P(z)K_x$ is the loop gain with the nominal model. Performance robustness can be defined as the sensitivity of the performance of the closed-loop system to process changes. The less sensitivity is, the larger performance robustness is. The sensitivity function of the closed-loop transfer function describing the tracking behavior with respect to changes in the open-loop transfer function becomes:

$$S_S(z)=\frac{\Delta_C(z)}{\Delta_o(z)}=\frac{1}{1+\hat{H}_L(z)} \tag{40}$$

$|\hat{H}_L(z)|$ or equivalently $|K_x|$ must be kept large in order to obtain small $|S_S(z)|$.

3.3.2 Robust stability

Robust stability is the ability of a closed-loop system to remain stable in the presence of modeling errors. It means that the controller which stabilizes the nominal model would stabilize a family of systems which exist in an uncertainty region around the nominal model.

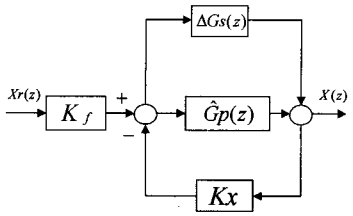

Fig. 9 A block diagram of the closed-loop system with a model uncertainty

Assume that there exists an additive model uncertainty $\Delta G_s(z)$. The actual plant model $G_p(z)$ can then be replaced by $G_p(z)=\hat{G}_p(z)+\Delta G_s(z)$. The closed-loop control block diagram with model uncertainty is shown in Fig. 9.

The transfer function can then be written as:

$$\frac{X(z)}{X_r(z)}=\frac{[\hat{G}_P(z)+\Delta G_S(z)]K_f}{(I+\hat{G}_P(z)K_x)\left(I+\dfrac{\Delta G_S(z)K_x}{I+\hat{G}_P(z)K_x}\right)} \tag{41}$$

where $X_r(z)$ is a reference. Since the feedback part K_x is chosen to stabilize the nominal plant, the denominator $I+\hat{G}_P(z)K_x$ satisfies the Nyquist criterion. A sufficient condition for stability of the design is then that the denominator $I+\dfrac{\Delta G_S(z)K_x}{I+\hat{G}_P(z)K_x}$ meets the Nyquist criterion, namely

$$\left|\frac{\Delta G_S(z)K_x}{I+\hat{G}_P(z)K_x}\right|\leq 1 \tag{42}$$

Due to the fact that $\left|\dfrac{\Delta G_S(z)K_x}{I+\hat{G}_P(z)K_x}\right|\leq|\Delta G_S(z)|\left|\dfrac{K_x}{I+\hat{G}_P(z)K_x}\right|$, Eq. (42) will be satisfied whenever $|\Delta G_S(z)|\left|\dfrac{K_x}{I+\hat{G}_P(z)K_x}\right|\leq 1$. The maximum size of $\Delta G_S(z)$, $|\Delta G_S(z)|_m$, is obtained by

$$|\Delta G_S(z)|_m=\frac{I+\hat{G}_P(z)K_x}{K_x} \tag{43}$$

The variation of the maximum size of the model uncertainty, $|\Delta G_S(z)|_m$ with the design parameters can be examined. It is also noted that robust stability conflicts with the effects on robust performance. The effects of the design parameters T_f to robust performance and robust stability are

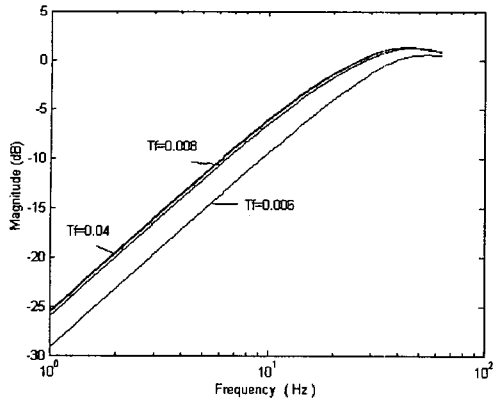

Fig. 10 Maximum singular values of sensitivity matrices, $\sigma(\mathrm{Ss}(z))$ of the closed-loop system with respect to T_f

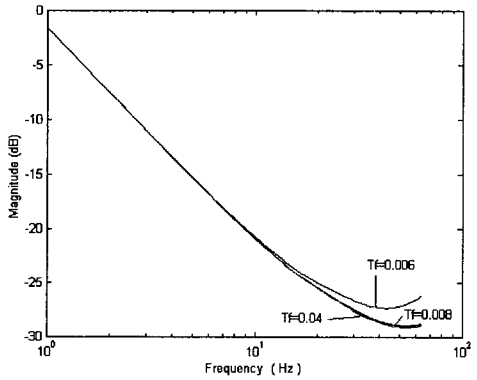

Fig. 11 Maximum singular values of maximum tolerable model uncertainties $\sigma(\Delta \mathrm{Gs}(z))$ of the closed-loop system with respect to T_f

shown in Figs. 10 and 11. The results indicate that a decrease in T_f results in an enhancement of robust performance, but an inverse influence on robust stability.

4. Conclusion

The tracking performance of a sliding horizon feedback/feedforward preview optimal control when applied to a hydraulic automotive motion simulator was described. The design was developed by solving an ordinary differential equation problem instead of a Ricatti equation which is necessary in the finite horizon case. Simulation results indicate that the proposed technique has good performance improvement in phase tracking when compared with the conventional design methods.

It was also concluded that the proposed design has more tuning flexibility comparing with the classical design since the variable horizon length offers another tuning parameter to achieve better design performance and robustness.

References

Brogan, W. L., 1985, *Modern Control Theory*, Prentice Hall Inc.

Cho, B. K., 1999, "Active Suspension Controller Design Using MPC with Preview Information," *KSME Int. Journal*, Vol. 13, No. 2, pp. 168~174.

Kirk, D. E., 1970, *Optimal Control Theory-An Introduction*, Prentice Hall Inc.

Kuehn, J., Liu, L., Shui, H. and Patten, W. N., 1993, "A Comparison of Robust Control Designs For A 3-Degree of Freedom Seat Simulator," DSC-Vol. 52, *Advanced Automotive Technologies*, ASME WAM, pp. 321~328.

Kuo, C. C., Wu, H. C., Yan, W. and Patten, W. N., 1993, "A Three Degree of Freedom Automobile Seat Simulator," DSC-Vol. 52, *Advanced Automotive Technologies*, ASME WAM, pp. 385~395.

Kwon, W. H. and Byun, D. G., 1989, "Receding Horizon Tracking Control as a Predictive Control and Its Stability Properties," *Int. J. of Control*, Vol. 50, No. 5, pp. 1806~1824.

Kwon, W. H., Choi, H., Byun, D. G. and Noh, S., 1992, "Recursive Solution of Generalized predictive Control and Its Equivalence to Receding Horizon Tracking Control," *Automatica*, Vol. 28, No. 6, pp. 1235~1238.

Lee, G. B., 1997, "A Receding Time Horizon Optimal Feedrate Control with Cross-Coupled Structure for Multiaxial Systems," *KSME Int. Journal*, Vol. 11, No. 4, pp. 419~427.

Lee, S. M., Bien, Z. and Park, S. O., 1990, "Online Optimal Terrain-Tracking System," *Optimal Control Applications and Methods*, Vol. 11, pp. 289~306.

Patten, W. N., Huang, J. and Wu, H. C., 1994,

"A Real Time Receding Horizon Preview Controller Design for Auto Suspensions," *ASME J. of Dynamic Systems*, Measurement and Control.

Patten, W. N., White, L. W. Kuo, C. C. and Wu, H. C., 1993, "A FEM Based Optimal Receding Horizon Control for Systems with Previewable Input," *ACC*, Vol. 2, pp. 1593 ~1597.

Shen, K., Liu, L., Mo, C., Sunwoo, M., and Patten, W. N., 1996, "Predictive Feedforward Control of an Electro-Hydraulic Automotive Seat Simulator," *13th IFAC World Congress*, San Francisco, USA, pp. 267~272.

Tomizuka, M. and Rosenthal, D. E., 1979, "On Optimal Digital State Feedback Controller with Integral and Preview Actions," *ASME J. of Dynamic Systems, Measurement and Control*, Vol. 101(2), pp. 172~178.

Yan, W., 1994, *A Study of Different Automatic Control Strategies for an Electro-Hydraulic Three Degree of Freedom Seat Motion Simulator*, MS thesis, University of Oklahoma.